

Biodistribution and toxicity assessment of radiolabeled and DMSA coated ferrite nanoparticles in mice

S. Fatahian · D. Shahbazi-Gahrouei · M. Pouladian ·
M. H. Yousefi · Gh. R. Amiri · A. Noori

Received: 10 March 2012 / Published online: 12 May 2012
© Akadémiai Kiadó, Budapest, Hungary 2012

Abstract DMSA-coated Fe_3O_4 nanoparticles were synthesized by wet-chemical method. The chemical interaction between Fe_3O_4 and DMSA were investigated by FTIR. They were directly radiolabeled with $^{99\text{m}}\text{Tc}$ radioisotope ($\text{Fe}_3\text{O}_4\text{@DMSA-}^{99\text{m}}\text{Tc}$) at room temperature in the presence of stannous solution as a reducing agent. Magnetic and structure properties of $\text{Fe}_3\text{O}_4\text{@DMSA-}^{99\text{m}}\text{Tc}$ nanoparticles were investigated by AGFM, TEM, and XRD. Biodistribution and toxicity assessment of $\text{Fe}_3\text{O}_4\text{@DMSA-}^{99\text{m}}\text{Tc}$ were studied in mice by intravenous and intraperitoneally injections, respectively. Blood, kidney, and liver factors were measured 4 days post injection and at the mean-while tissue sections were prepared from their kidney and liver. The results indicate that, the $\text{Fe}_3\text{O}_4\text{@DMSA-}^{99\text{m}}\text{Tc}$ nanoparticles were passed through the membrane of different cells but do not create any disorder in the kidney and liver function even in high doses such as 300 mg/kg.

Keywords Fe_3O_4 nanoparticle · Radio labeling · DMSA coated · Biodistribution · Toxicity · $^{99\text{m}}\text{Tc}$

S. Fatahian (✉) · M. Pouladian
Department of Medical Radiation Engineering, Science and Research Branch, Islamic Azad University, Tehran, Iran
e-mail: fatahian@iaufala.ac.ir

D. Shahbazi-Gahrouei
Department of Medical Physics, School of Medicine,
Isfahan University of Medical Sciences, Isfahan, Iran

M. H. Yousefi
Department of Sciences, Nano-Center, Malek-Ashtar University
of Technology, Shahin-Shahr, P.O. Box 83145/115, Isfahan, Iran

Gh. R. Amiri · A. Noori
Falavarjan Branch, Islamic Azad University, Isfahan, Iran

Introduction

High proportion of surface to volume of the nanoparticles in comparison of bulk samples, have made them adequate to be used in many medical and industrial applications. There are extensive researches on wide application of Fe_3O_4 nanostructures such as MR imaging tumor therapy [1], drug delivery and gene transfer to tissues and cells [2], labeling cells, and macromolecules [3]. There are many methods which can be used for synthesizing Fe_3O_4 and other nanoparticles such as gamma-irradiation [4], electron beam radiation [5], co-precipitation, low temperature solid state reaction, and microwave method [6–10].

Nanoparticles are often smaller than cellular structures, virus, protein, or a gene. This unique characteristic provided them proper for quick distribution in most organs and tissues, and therefore very strong cellular uptake phenomenon [11]. In recent years, in order to increase the stability of nanoparticles in biological systems and blood circulation, they are coated with biocompatible materials such as albumin, dextran [12], polyethylene glycol, polyethylene oxide [13], aspartic acid, and dimercaptosuccinic acid (DMSA) ($\text{C}_4\text{S}_2\text{O}_4\text{H}_6$) [14]. Presence of such coatings increases the entrance to cells and decreases the toxicity effects [15].

There are few reports on Fe_3O_4 toxicity especially under in vivo conditions and moreover some researchers showed controversial results. For instance, some studies have reported minimal toxicity in some concentrations and some others have shown non-toxicity effects under in vivo conditions [16–18]. Therefore, it is essential to assess the toxicity effects of Fe_3O_4 nanoparticles in both in vitro and in vivo conditions. Moreover, considering the variety of biocompatible compounds can be used, it is interesting to study the tissue distribution and Fe_3O_4 toxicity for any particular coating compounds separately [15].

DMSA is a nontoxic substance that nowadays is used in some patients to absorb additional elements of the body (chelating agent) [16]. Using this substance creates an anionic coating around the nanoparticle surface and prevents opsonization (accumulation of blood proteins around the nanoparticle). Therefore, DMSA helps nanoparticles for less deletion by reticuloendothelial system of liver and spleen. Presence of this substance on nanoparticles surface increases the cell absorption and tissue distribution and also decreases direct contact with cells and cellular components which led to reduction of toxicity effects [18].

On the other hand, Technetium-99m (^{99m}Tc) is one of the most important radioisotopes in nuclear medicine which has wide application [19]. Radiolabeling of coated Fe_3O_4 with ^{99m}Tc can potentially help to achieve more desirable tissue distribution by applying magnetic fields due to super paramagnetic properties of Fe_3O_4 nanoparticles [20]. Radiolabeling of nanoparticles may reduce their effects on biodistribution and toxicity. In this study an attempt is to produce the coated Fe_3O_4 nanoparticles which labeled with ^{99m}Tc and also assess the biodistribution and toxicity effect of the nanoparticles in mice. At the end, in vitro and in vivo stability of final prepared nanoparticles also were investigated.

Experimental

Synthesis of DMSA coated Fe_3O_4 nanoparticles

DMSA-coated Fe_3O_4 nanoparticles ($\text{Fe}_3\text{O}_4@$ DMSA) were synthesized by wet-chemical method. For this purpose, three solutions of FeCl_2 (0.01 M), FeCl_3 (0.02 M), and NaOH (0.08 M) (all from Merck Company) were prepared in the distilled deionized water, under vigorous stirring. At first, FeCl_2 solution was poured into a three spout balloon container. Meanwhile, FeCl_3 solution was added to the same balloon. After that, 0.01 M DMSA solution was prepared in deoxygenated deionized water. In the construction process, every 3 or 4 s, one droplet of DMSA solution was added via nitrogen bubbling and magnetic stirrer. Finally, FeCl_3 solution was added to the balloon by the same way and under atmosphere control condition (N_2). The resulting solution was washed by deionized water and then was centrifuged in order to remove any impurity aggregate. Then, the precipitated sample was dried at room temperature. All processes were done at room temperature. The details are described in references [21, 22].

Radiolabeling of $\text{Fe}_3\text{O}_4@$ DMSA with ^{99m}Tc radioisotope

In the present study, in order to radiolabeling of $\text{Fe}_3\text{O}_4@$ DMSA nanoparticles, the ^{99m}Tc , with activity of

1.3 GBq was prepared from $^{99}\text{Mo}-^{99m}\text{Tc}$ generator. It was injected into a small sterile and vacuuming vial under the observance of radiation protection rules. Subsequently, 0.5 ml of stannous chloride (2.0 mg/ml) solution in 0.1 N HCl, was injected into the same vial, and stirred for several seconds. The stannous chloride, which mainly contains SnCl_2 , is a reducing agent that reduces surface charge of ^{99m}Tc to a suitable condition for labeling with other molecules. Then, 1 ml diluted $\text{Fe}_3\text{O}_4@$ DMSA solution was added into the vial containing ^{99m}Tc and stannous chloride. The mixture was kept at room temperature and radio labeled and coated Fe_3O_4 nanoparticles ($\text{Fe}_3\text{O}_4@$ DMSA- ^{99m}Tc) were prepared after several minutes. The details are described in references [23, 24].

Quality assurance of $\text{Fe}_3\text{O}_4@$ DMSA- ^{99m}Tc

The chemical interaction between Fe_3O_4 and DMSA were investigated by Fourier transform infrared spectroscopy (FTIR, JASCO FT/IR-680 PLUS). The labeling efficiency was assessed by instant thin layer chromatography (ITLC) which silica gel and acetone solvent were used as instant and mobile phase, respectively. The radioactivity of each part of ITLC strips was determined by High Purity Germanium spectroscopy (HPGe spectroscopy, Canberra). Magnetic and structure properties of $\text{Fe}_3\text{O}_4@$ DMSA- ^{99m}Tc nanoparticles were investigated by alternating gradient-force magnetometer (AGFM, Meghnatis Daghigh Kavir Co, Iran) and X-ray diffraction (XRD, Bruker D8 ADVANCE $\lambda = 0.154$ nm Cu $K\alpha$ radiation) [22].

Breeding animals and treatments

The animal studies were performed in accordance with regulatory guidance's on the care and use of experimental animals. For this purpose, 55 male and female mice of Balb/C strain were provided from RAZI Vaccine and Serum Research Institute. Studying their life cycle was performed in natural light and humid and at 22–24 °C temperature. In order to investigate the toxicity effects 25 mice were randomly selected. They were divided into five equal groups. Four groups were intraperitoneally injected by 50, 100, 200, and 300 mg/kg of $\text{Fe}_3\text{O}_4@$ DMSA- ^{99m}Tc , respectively, and 5th group just was injected with normal saline (control group). Rest mice were used for biodistribution and stability assessments.

In vitro and in vivo stability

In order to assessment of in vivo stability, 100 MBq of $\text{Fe}_3\text{O}_4@$ DMSA- ^{99m}Tc intravenously injected to five mice (each mouse received 100 MBq). After that blood samples were collected at different time intervals which were then

subjected to ITLC. For In vitro stability investigation, 50 MBq of $\text{Fe}_3\text{O}_4\text{@DMSA-}^{99\text{m}}\text{Tc}$ were mixed separately to saline and mice serum and then incubated at 37 °C. Samples were subjected to ITLC at different time intervals.

Measurement of blood, kidney, and liver factors

Four days after treatment, blood samples were taken directly from heart under mild anesthesia with ether. Samples were poured into the special pipes which contain edetic acid (EDTA) anti coagulation agent. After that, cell blood counting (CBC) test was done (Sysmex K-100) for all blood samples in order to assessment the number and percentage of red blood cells, white blood cells, platelets, neutrophils, and lymphocytes. Kidney and liver factors such as lactate dehydrogenase (LDH), serum glutamic pyruvate transaminase (SGPT), serum glutamic oxaloacetic transaminase (SGOT), uric acid, creatinine, and urea were measured by Hitachi Automatic Analyzer (Roche 902).

Tissue section preparation for Perl's method staining

For this purpose, several mice were dissected immediately after bleeding (4 days after treatment) and tissue sections were prepared from their kidney and liver. These organs were selected because the liver is the center of drug metabolism and kidneys are responsible for drug exclusion from the blood circulation. Then, the prepared tissue sections were stained using specific iron Prussian blue method (Perl's Method) to observe nanoparticles accumulation. Accumulation of iron oxide nanoparticles were showed in tissue sections as dark blue grains under microscope light.

Biodistribution of $\text{Fe}_3\text{O}_4\text{@DMSA-}^{99\text{m}}\text{Tc}$

For evaluating localization of $\text{Fe}_3\text{O}_4\text{@DMSA-}^{99\text{m}}\text{Tc}$ in different tissues and organs, 25 mice were divided into five equal groups that each group contains five mice. Each mouse was intravenously injected through the tail vein with 200 kBq of $\text{Fe}_3\text{O}_4\text{@DMSA-}^{99\text{m}}\text{Tc}$. The tissue distribution studies were evaluated after 20 min, 1, 2, 4, and 10 h post injection. At these time intervals, animals were sacrificed and subsequently, tissues (brain, lung, spleen, kidney, liver, and blood) were removed and washed with normal saline. The radioactivity of each organ was counted with Gamma counter (Berthold-LB2111, Germany) and showed as percent injected dose per gram of tissue [25].

Statistical analysis

The mean values of blood, kidney, and liver factors (with treatment dose segregation) were compared by ANOVA

test (analysis of variance) and *t* test by SPSS (version 15) computer program in all groups. Results are the mean of five separate experiments for each group.

Results and discussion

Physical properties assessment and quality assurance of $\text{Fe}_3\text{O}_4\text{@DMSA-}^{99\text{m}}\text{Tc}$

Figure 1 shows the transmission electron microscope (TEM) photograph of the $\text{Fe}_3\text{O}_4\text{@DMSA}$ nanoparticles. This picture demonstrates that the size of the particles is around 10–15 nm with approximately uniform size distribution. The mean size of the nanoparticles was also determined from XRD pattern by Debye–Scherer formula. It was calculated around 15 nm which has good agreement with that TEM result (XRD curve is not shown here) [22].

Magnetic properties of the nanoparticles were assessed by AGFM and it was found that they have the super paramagnetic property. The saturation magnetization was determined by extrapolation of magnetization curve on the basis of $1/H$ when $1/H \rightarrow 0$. It was measured 24 emu/g (AGFM curve is not shown here) [22].

Figure 2 indicates the FTIR curve of the Fe_3O_4 , DMSA, and $\text{Fe}_3\text{O}_4\text{@DMSA}$. As can be seen, in the Fe_3O_4 curve, 1,628 and 3,419 peaks are related to OH junctions and it means that there is water in the material structure. The 581 peak shows that the spinel structure was formed and we will see it has a good agreement with XRD results. On the other hand, in the $\text{Fe}_3\text{O}_4\text{@DMSA}$ curve, 1,619 and 1,376 peaks are related to the asymmetry and symmetry stresses of COO group, respectively. If we compare them with the 1,699 and 1,421 peaks in the DMSA curve, it can be concluded that the DMSA has coated the surface of the Fe_3O_4 nanoparticles. Also, decrease in the 581 peak is the other reason for this conjunction [22].

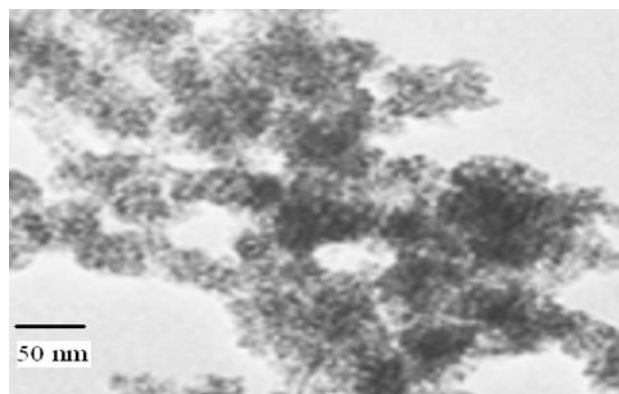


Fig. 1 TEM photograph of the $\text{Fe}_3\text{O}_4\text{@DMSA}$ nanoparticles

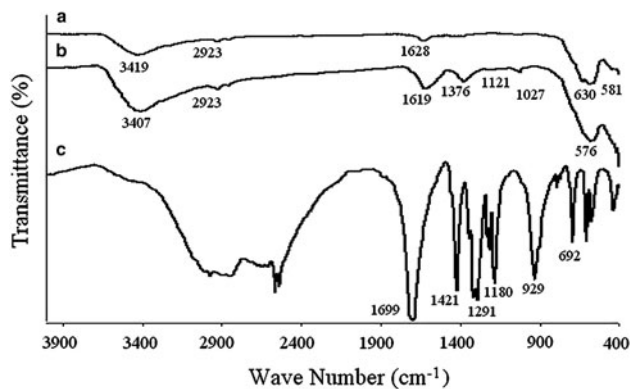


Fig. 2 **a** FTIR curve of Fe_3O_4 . **b** FTIR curve of Fe_3O_4 @DMSA. **c** FTIR curve of DMSA

The labeling efficiency of nanoparticles was verified by using ITLC method, since it is an easy way and well accepted process to assess the radiolabeling quality in nuclear medicine. The labeling efficiency was obtained more than 98 %. The same ITLC tests were done after 2, 4, and 8 h and the labeling efficiency of 90 % was determined.

In vitro and in vivo stability studies

In vitro stability study indicated that the labeled conjugate was approximately stable up to 10 h both in serum (around 88 %) and normal saline (around 90 %) which had good agreement with the in vivo stability studies (around 92 %).

Results of blood, kidney, and liver factors measurement

Table 1 shows the results of CBC tests 4 days after treatment. As can be seen, the WBC and lymphocyte mean numbers are decreased for samples treated over 100 mg/kg concentration. The similar event has happened for RBC mean number over 200 mg/kg and for platelets just in 300 mg/kg concentration. On the other hand, neutrophil percentage is slowly increased for all treatment doses.

The results of kidney and liver factors 4 days after treatment are shown in Table 2. By considering the *P* value which is more than 0.05 for all variables, it can be seen that, there is not any meaningful difference for kidney and liver factors (such as LDH, SGPT, SGOT, Uric Acid, Creatinine, and Urea) between the treated and control groups in all treatment doses. This point means that Fe_3O_4

Table 1 Cell Blood Counting (CBC) test 4 days after treatment with coated and radio labeled Fe_3O_4 nanoparticles (intraperitoneally injection)

Dose mg/kg	WBC $\times 10^3$ per μl	RBC $\times 10^3$ per μl	Platelets $\times 10^3$ per μl	Lymphocyte $\times 10^3$ per μl	Lymphocyte percentage	Neutrophil percentage
Control	4.64 \pm 0.68	10.05 \pm 0.81	531 \pm 54	2.96 \pm 0.56	59 \pm 6	40 \pm 5
50	4.56 \pm 0.73	10.07 \pm 0.76	563 \pm 45	2.85 \pm 0.55	56 \pm 5	42 \pm 5
100	2.73 \pm 0.62	10.09 \pm 0.99	589 \pm 72	1.68 \pm 0.23	55 \pm 4	44 \pm 4
200	2.37 \pm 0.53	7.35 \pm 1.63	585 \pm 59	1.09 \pm 0.21	54 \pm 3	45 \pm 3
300	1.43 \pm 0.40	7.11 \pm 1.19	179 \pm 35	0.90 \pm 0.19	47 \pm 2	52 \pm 2
	$P \geq 0.01$	$P \geq 0.01$	$P \geq 0.01$	$P \geq 0.01$	$P \geq 0.05$	$P \geq 0.05$

Results are the mean \pm SD of five separate experiments

Table 2 Results of kidney and liver factors measurement 4 days after treatment with coated and radio labeled Fe_3O_4 nanoparticles (intraperitoneally injection)

Dose (mg/kg)	Urea (mg/dl)	Creatinine (mg/dl)	Uric acid (mg/dl)	SGOT	SGPT	LDH	Albumin
Control	60 \pm 7	0.35 \pm 0.08	0.76 \pm 0.09	160 \pm 6	61 \pm 3	1,138 \pm 21	3.08 \pm 0.12
50	61 \pm 7	0.41 \pm 0.06	0.79 \pm 0.08	129 \pm 7	60 \pm 2	988 \pm 32	2.38 \pm 0.28
100	56 \pm 8	0.40 \pm 0.05	0.75 \pm 0.08	130 \pm 6	69 \pm 3	1,096 \pm 30	3.13 \pm 0.14
200	66 \pm 10	0.42 \pm 0.08	0.84 \pm 0.09	138 \pm 7	77 \pm 3	994 \pm 36	2.38 \pm 0.13
300	60 \pm 17	0.45 \pm 0.10	0.67 \pm 0.06	155 \pm 7	68 \pm 4	992 \pm 51	2.80 \pm 0.09
	$P \geq 0.05$	$P \geq 0.05$	$P \geq 0.05$	$P \geq 0.05$	$P \geq 0.05$	$P \geq 0.05$	$P \geq 0.05$

SGOT serum glutamic oxaloacetic transaminase

SGPT serum glutamic pyruvate transaminase

LDH lactate dehydrogenase

Results are the mean \pm SD of five separate experiments

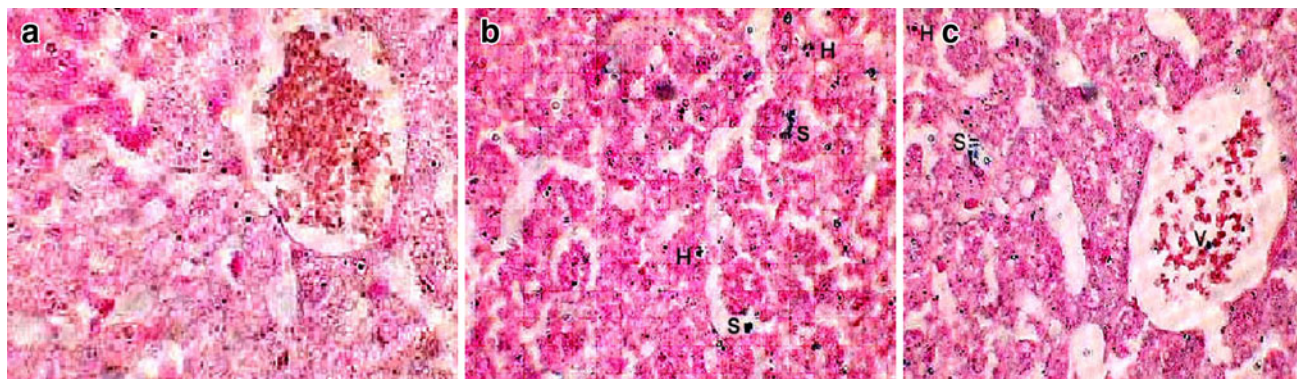


Fig. 3 The stained liver tissue sections (Perl's method) 4 days after treatment (Magnification $\times 40$). **a** Control group. **b, c** 50 mg/kg treated group. Dark blue dots show the accumulation of iron oxide

nanoparticles in the sinusoids (S), hepatocytes (H) and liver blood vessels (V). (Color figure online)

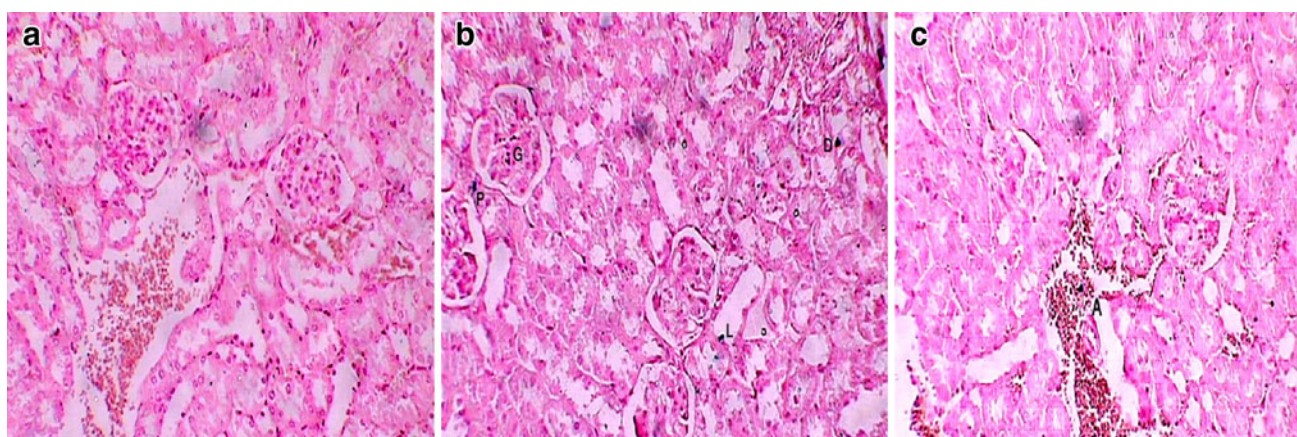


Fig. 4 The stained kidney tissue sections (Perl's method) 4 days after treatment (Magnification $\times 40$). **a** Control group. **b, c** 50 mg/kg treated group. Dark blue dots show the accumulation of iron oxide

nanoparticles in the glomerules (G), nephron wall cells (P & D), internal nephron canal (L) and kidney blood vessels (V). (Color figure online)

nanoparticles do not create any disorder in the kidney and liver function even in high doses (300 mg/kg).

Stained kidney and liver tissue sections observation

Figure 3, displays aggregated $\text{Fe}_3\text{O}_4\text{@DMSA-}^{99\text{mTc}}$ nanoparticles in the stained liver tissue sections 4 days after treatment. As can be seen, these nanoparticles were detected in the sinusoids and hepatocytes of the liver tissue of treatment mice.

Figure 4 shows accumulated $\text{Fe}_3\text{O}_4\text{@DMSA-}^{99\text{mTc}}$ nanoparticles in the stained kidney tissue sections 4 days after treatment. It can be seen that they were found in the glomerules, nephron wall cells, internal nephron canal, and kidney blood vessels. These results indicate that, the $\text{Fe}_3\text{O}_4\text{@DMSA-}^{99\text{mTc}}$ nanoparticles were passed through the membrane of different cells.

Biodistribution of $\text{Fe}_3\text{O}_4\text{@DMSA-}^{99\text{mTc}}$ in normal mice

Tissue distribution of $\text{Fe}_3\text{O}_4\text{@DMSA-}^{99\text{mTc}}$ between 20 min and 10 h in healthy mice of Balb/c is represented in Table 3. As can be seen, the major accumulation is observed in liver. The second organs which have high accumulation are kidneys, lungs, and spleen. There is considerable difference between their accumulations with that of liver. Negligible uptake is found in brain. Liver and lung indicated a reduction accumulation after 20 min whereas spleen and kidney showed an increased uptake after 2 h post injection and then decreased. High accumulation of liver is related to the phagocytic uptake in the Kupffer cell of the liver. Many studies reported that most of the intravenously injected particles are removed from blood circulation by the mononuclear phagocyte system

Table 3 Biodistribution of Fe₃O₄@DMSA-^{99m}Tc in mice following intravenous injection

Organ	Time after injection (injected dose percentage per gram of tissue)				
	20 min	1 h	2 h	4 h	10 h
Liver	2.54 ± 0.24	2.04 ± 0.22	1.52 ± 0.20	1.08	0.15
Kidney	0.23 ± 0.03	0.35 ± 0.04	0.54 ± 0.06	0.37	0.09
Lung	0.27 ± 0.04	0.15 ± 0.02	0.11 ± 0.01	0.09	0.004
Spleen	0.25 ± 0.03	0.54 ± 0.06	0.76 ± 0.08	0.49	0.11
Brain	0.01 ± 0.002	0.008 ± 0.001	0.006 ± 0.001	0.005	0.001
Blood	0.30 ± 0.03	0.16 ± 0.02	0.11	0.05	0

Results are the mean ± SD of five separate experiments

(MPS) [16, 17]. The result is in accordance with the earlier reports which shown Fe₃O₄ localization coating with other biocompatible materials or labeling with other radioisotopes [24, 26].

Conclusions

From the Figs. 3, 4 it is concluded that, the Fe₃O₄@DMSA-^{99m}Tc nanoparticles were passed through the membrane of different cells and dramatically penetrate to liver and kidney after 4 days. But they did not create any abnormality or functional disorder in the kidney and liver tissues.

From Table 2 it is found that, there is not any meaningful variation in the liver and kidney enzymes or factors even in high treatment doses such as 300 mg/kg ($P \geq 0.05$). This is probably for the reason that nanoparticles were eliminated slowly from the body by excretion or may be lack of absorption.

On the other hand, the number and percentage of different blood cells were decreased specially in high doses. It is noteworthy that these high doses never used in medicine especially for diagnostic applications and as we know ^{99m}Tc only used for diagnostic applications.

From findings here, there is not any serious harmful side effect for Fe₃O₄@DMSA-^{99m}Tc nanoparticles in order to in vivo applications.

Acknowledgments The authors are grateful from Department of Biology, Faculty of Basic Sciences, Falavarjan Islamic Azad University for their cooperation and supplying the experimental equipments (Most experimental results are from research code No. 301/2811).

References

- Weissleder R, Elizondo G, Wittenburg J, Rabito CA, Bengel HH, Josephson L (1990) Ultrasmall superparamagnetic iron oxide: characterization of a new class of contrast agents for MR imaging. *J Radiology* 175:489–493
- Pankhurst QA, Connolly J, Jones SK, Dobson J (2003) Applications of magnetic nanoparticles in biomedicine. *J Phys D Appl Phys* 36:167–181
- Molday RS, MacKenzie D (1982) Immunospesific ferromagnetic iron dextran reagents for the labeling and magnetic separation of cells. *J Immunol Methods* 52:353–367
- Gracien EB, Ruimin Z, LiHui X, Kanza Kanza L (2006) Effects of pH on the morphology of iron oxides synthesized under gamma-irradiation. *J Radioanal Nucl Chem* 270:473–478
- Zhang X, Zhou R, Rao W (2006) Influence of precipitator agents NaOH and NH₄OH on the preparation of Fe₃O₄ nano-particles synthesized by electron beam irradiation. *J Radioanal Nucl Chem* 270:285–289
- Amiri GhR, Yousefi MH, Aboulhassani MR, Keshavarz MH, Shahbazi D, Fatahian S, Alahi M (2010) Radar absorption of Ni_{0.7}Zn_{0.3}Fe₂O₄ nanoparticles. *Dig J Nanomater Bios* 5(3): 1025–1031
- Amiri GhR, Yousefi MH, Aboulhassani MR, Keshavarz MH, Manouchehri S, Fatahian S (2011) Magnetic properties and microwave absorption in Ni–Zn and Mn–Zn ferrite nanoparticles synthesized by low-temperature solid-state reaction. *J Magn Mater* 323:730–734
- Jelvani AR, Amiri GhR, Fatahian S, Manouchehri S, Habibi M, Mousarezaei R (2011) Magnetic properties comparison of Co_{0.5}Zn_{0.5}Fe₂O₄ nanoparticles prepared by different methods. *J Optoelectronics Adv Materials-Rapid Communications* 5(11): 1216–1218
- Amiri GhR, Yousefi MH, Fatahian S (2012) Magnetic properties of CoFe₂O₄ and Co_{0.5}Zn_{0.5}Fe₂O₄ ferrite nanoparticles synthesized by microwave method. *J Optoelectronics Adv Materials-Rapid Communications* 6(12):158–161
- Chen Z, Meng H, Yuan H, Xing G, Chen C, Zhao F, Wang Y, Zhang C, Zhao Y (2007) Identification of target organs of copper nanoparticles with ICP-MS technique. *J Radioanal Nucl Chem* 272(3):599–603
- Salata OV (2004) Applications of nanoparticles in biology and medicine. *J Nanobiotech* 2:3
- Berry CC, Wells S, Charles S, Curtis ASG (2003) Dextran and albumin derivatised iron oxide nanoparticles: influence on fibroblasts in vitro. *Biomaterials* 24:4551–4557
- Lacava LM, Lacava ZGM, Da Silva MF, Silva O, Chaves SB, Azevedo RB et al (2001) Magnetic resonance of a dextran-coated magnetic fluid intravenously administered in mice. *Biophys J* 80:2483–2486
- Sadeghiani N, Barbosa LS, Silva LP, Azevedo RB, Morais PC, Lacava ZGM (2005) Genotoxicity and inflammatory investigation in mice treated with magnetite nanoparticles surface coated with polyaspartic acid. *J Magn Mater* 289:466–468
- Shubayev VI, Pisanic TR, Jin S (2009) Magnetic nanoparticles for theragnostics. *Adv Drug Delivery Rev* 61:467–477

16. Garcia MP, Parca RM, Chaves SB, Silva LP, Santos AD, Lacava ZGM et al (2005) Morphological analysis of mouse lungs after treatment with magnetite-based magnetic fluid stabilized with DMSA. *J Magn Magn Mater* 293:277–282
17. Hafeli UO, Pauer GJ (1999) In vitro and in vivo toxicity of magnetic microspheres. *J Magn Magn Mater* 194:76–82
18. Kim JS, Yoon TJ, Yu KN, Kim BG, Park SJ, Kim HW et al (2006) Toxicity and tissue distribution of magnetic nanoparticles in mice. *Toxicol Sci* 89(1):338–347
19. Hnacell C (2008) Nuclear medicines double hazard: Imperiled treatment and the risk of terrorism. *Nonproliferation Rev* 15(2): 185–208
20. Fu CM, Wang YF, Guo YF, Lin TY, Chiu JSh (2005) In Vivo biodistribution of intravenously injected ^{99m}Tc labeled ferrite nanoparticles bounded with biocompatible medicals. *IEEE Trans Magn* 41(10):4120–4122
21. Pisanic TR, Blackwell JD, Shubayev VI, Finones RR, Jin S (2007) Nanotoxicity of iron oxide nanoparticle internalization in growing neurons. *Biomaterials* 28:2572–2581
22. Fatahian S, Shahbazi D, Pouladian M, Yousefi MH, Amiri GhR, Shahi Z, Jahanbakhsh H (2011) Preparation and magnetic properties investigation of Fe_3O_4 nanoparticles ^{99m}Tc labeled and Fe_3O_4 nanoparticles DMSA coated. *Dig J Nanomater Bios* 6(3):1161–1165
23. Fu CM, Wang YF, Chao YC, Huang HS, Yang MD (2004) Directly labeling ferrite nanoparticles with Tc-99m radioisotope for diagnostic applications. *IEEE Trans Magn* 40(4):3001–3003
24. Banerjee T, Singh AK, Sharma RK, Maitra AN (2005) Labeling efficiency and biodistribution of Technetium-99m labeled nanoparticles: interference by colloidal tin oxide particles *International. J Pharmaceutics* 289:189–195
25. Singh AK, Verma J, Bhatnagar A, Sen S, Bose M (2003) A specific agent for diagnosis of tuberculosis. *World J Nucl Med* 2:292–305
26. Jalilian AR, Hosseini L, Mahmoudi M, Yousefnia H, Majdabadi A, Pouladian M (2011) Preparation and biological evaluation of radiolabeled-folate embedded superparamagnetic nanoparticles in wild-type rats. *J Radioanal Nucl Chem* 287:119–127